

Studies on Magnetic Properties of $\text{UO}_2\text{-CeO}_2$ Solid Solutions

I. Magnetic Susceptibilities of Solid Solutions with Low Cerium Concentrations

YUKIO HINATSU AND TAKEO FUJINO

*Department of Chemistry, Japan Atomic Energy Research Institute,
Tokai-mura, Ibaraki 319-11, Japan*

Received March 23, 1987

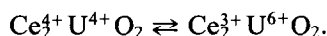
Magnetic susceptibilities of $\text{Ce}_y\text{U}_{1-y}\text{O}_2$ solid solutions were measured from 4.2 K to room temperature and compared with those of $L_y\text{U}_{1-y}\text{O}_2$ ($L = \text{Th, Zr, Y, La, Pr, Nd}$) solid solutions. An antiferromagnetic transition was observed for the solid solutions with $y \leq 0.35$. The Néel temperature (T_N) decreases gradually with increasing y until $y = 0.30$, and above this value it decreases more rapidly. The critical concentration of antiferromagnetism for $\text{Ce}_y\text{U}_{1-y}\text{O}_2$ solid solutions was estimated to be $y = 0.40$. Below T_N , after a little decrease, the susceptibility increases again with decreasing temperature. It is found that the substitution of Ce^{4+} for U^{4+} in UO_2 lattice results in not only magnetic dilution of UO_2 , but also oxidation of some uranium ions to pentavalent state (with reduction of the corresponding amount of Ce^{4+} ions to Ce^{3+}), i.e., some transfer of an electron between uranium and cerium ions is considered to occur. © 1988 Academic Press, Inc.

Introduction

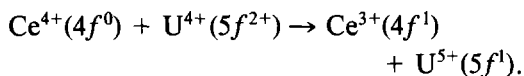
Studies on the uranium-cerium-oxygen system are important in nuclear-fuel chemistry because cerium shows some similarities in chemical properties to plutonium in the mixed oxide with uranium, which is used as a fuel in fast breeder reactors.

There have been numerous studies on this system. An interesting point is that some $\text{UO}_2\text{-CeO}_2$ solid solutions crystallize in a blue color known as "cerium-uranium blue." Hofmann and Höschele (1) first reported the preparation of this deep blue "cerium-uranium blue", having the composition near to Ce_2UO_6 . Because UO_2 is brown and CeO_2 is pale yellow, they as-

cribed the blue color of the mixed oxides to be due to the oscillation of the valence,



Later researchers have shown that UO_2 and CeO_2 form a continuous series of solid solutions and that the Ce_2UO_6 composition ($\text{Ce}:\text{U} = 2:1$) is but one unexceptional example of the solid solutions showing cerium-uranium blue (2, 3). Robin and Day (4) considered that U^{6+} ion is not an appropriate form of the uranium ion in cubic fluorite lattice because it tends to bond strongly with two oxygen ions to form the uranyl ion UO_2^{2+} . They argued that the blue color was due to the transfer of an electron between Ce^{4+} and U^{4+} ,



The phase relation and thermodynamics of this system have been extensively examined by many researchers (5–11). However, no magnetic studies have been carried out yet.

Uranium dioxide (UO_2) is a paramagnetic compound with two unpaired $5f$ electrons and changes to the antiferromagnetic state below $T_N = 30.8$ K (T_N , the Néel temperature). Its antiferromagnetism is of type I, and the magnetic moments of uranium ions are in the planes of the ferromagnetic layers perpendicular to a crystal axis; the moments of each plane are antiparallel to those of the neighboring planes (12). Another fact is that the paramagnetic–antiferromagnetic transition is first order (12). On the other hand, cerium dioxide (CeO_2) is diamagnetic.

In preceding papers, we have reported the magnetic properties of $(U, L)O_2$ solid solutions, L being Th, Zr, Y, La, Pr, or Nd. From the measurements of magnetic susceptibility of $(U, Th)O_2$ or $(U, Zr)O_2$ solid solutions (13–15), UO_2 was found to be magnetically diluted with diamagnetic ThO_2 or ZrO_2 , and the Néel temperature decreased linearly with decreasing uranium concentration. In $(U, Y)O_2$ or $(U, La)O_2$ solid solution, the substitution of Y^{3+} or La^{3+} for U^{4+} in UO_2 lattice resulted in not only magnetic dilution of UO_2 , but also oxidation of uranium ions from U^{4+} to the U^{5+} state in order to maintain electrical neutrality (16, 17). With increasing Y^{3+} or La^{3+} concentration, the Néel temperature decreased more rapidly at low concentrations than at high concentrations. In $(U, Pr)O_2$ or $(U, Nd)O_2$ solid solutions, UO_2 is not magnetically diluted with Pr^{3+} or Nd^{3+} ions, although some uranium ions are oxidized to the pentavalent state due to the substitution of these rare-earth ions for U^{4+} . The magnetic susceptibilities of $(U,$

$Pr)O_2$ or $(U, Nd)O_2$ solid solutions with low Pr^{3+} or Nd^{3+} concentrations (below 7 mole%) increased with decreasing temperature down to ca. 31 K and showed a discontinuous drop immediately below that temperature (18, 19).

In the present study, nearly oxygen-stoichiometric $(U, Ce)O_2$ solid solutions were prepared and their magnetic susceptibilities were measured from liquid helium temperature to room temperature. The results were compared with those of the above-mentioned $(U, L)O_2$ solid solutions and the electronic state of uranium in the solid solutions was examined.

Experimental

1. Sample Preparation

As starting materials, UO_2 and CeO_2 were used. Before use, UO_2 was reduced to the stoichiometric composition in flowing hydrogen at 1000°C, and CeO_2 was heated in air at 850°C to remove any moisture.

The UO_2 and CeO_2 were weighed to the intended atom ratios of uranium and cerium. After being finely ground in an agate mortar, the mixtures (~1.5 g) were pressed into pellets and then sealed in evacuated platinum ampoules with volume about 0.8 ml. The platinum ampoules were heated at 1500°C for >80 hr.

2. Analysis

2.1. X-ray diffraction analysis. An X-ray diffraction study was performed with $CuK\alpha$ radiation on a Phillips PW-1390 diffractometer equipped with a curved graphite monochromator. The lattice parameter of the samples was determined by the Nelson–Riley extrapolation method (20) applied to the diffraction lines above 80° (2 θ).

2.2. Determination of oxygen content. The oxygen nonstoichiometry in the solid solutions was determined by the back-

titration method (21, 22). A weighed amount of sample was dissolved in excess cerium(IV) sulfate solution. The cerium(IV) sulfate solution was standardized with stoichiometric UO_2 . The excess cerium(IV) was titrated against standard iron(II) ammonium sulfate solution with ferroin indicator. The oxygen amount was determined for predetermined Ce/U ratio.

3. *Magnetic susceptibility measurement.* Magnetic susceptibility was measured by a Faraday-type torsion balance in the temperature range from liquid helium temperature to room temperature. The apparatus was calibrated with Mn-Tutton's salt ($\chi_g = 10,980 \times 10^{-6}/(T + 0.7)$) used as a standard. The temperature of the sample was measured by a "normal" Ag vs Au-0.07 at% Fe thermocouple (23) (4.2–40 K) and an Au-Co vs Cu thermocouple (10 K to room temperature). Rapid thermal equilibrium was attained around the sample by introducing helium gas into the system up to ca. 10 mm Hg. To examine the field dependence, the magnetic susceptibilities were measured in each of the field strengths of 4,700, 6,900, 9,000, and 10,600 Gauss. To correct the magnetic susceptibilities for the samples, measurements were also made for the blank quartz tube under the same conditions. Details of the experimental procedure have been described elsewhere (14).

Results and Discussion

1. Lattice Parameter and Oxygen Nonstoichiometry

According to the reports by Markin *et al.* (5) and other researchers (7, 9), a solid solution $\text{Ce}_y\text{U}_{1-y}\text{O}_{2+x}$ with $y > 0.35$ and an oxygen/metal ratio below 2 results in the formation of two fluorite phases ($\text{MO}_{2.00} + \text{MO}_{2-x}$) below a certain temperature, which depends on x and y . In the present experiments, the samples were rapidly cooled in an electric furnace after heating at 1500°C.

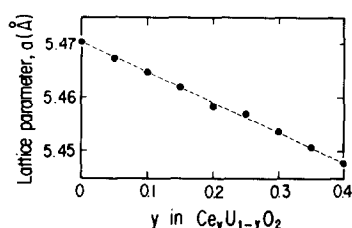


FIG. 1. Variation of lattice parameters with cerium concentration.

X-ray diffraction analysis showed that cubic, single-phase solid solutions with the fluorite structure were formed for all the specimens in this study.

The oxygen/metal ratios of the solid solutions, as determined by the cerium back-titration method, were nearly two.

The variation of lattice parameter with cerium concentration is shown in Fig. 1. The lattice parameter of the solid solutions decreases linearly with increasing cerium concentration, which satisfies Vegard's law at least in the experimental range of cerium concentration. This is consistent with the results of Rüdorff and Valet (2) and Markin *et al.* (5).

2. Magnetic Susceptibility

The temperature dependence of inverse magnetic susceptibilities per mole of uranium for the present solid solutions is shown in Figs. 2 and 3. An antiferromagnetic transition can be observed for the solid solutions with $y \leq 0.35$. The Néel temperature, T_N , decreases with increasing cerium concentration (y). Figures 4 and 5 closely represent the temperature dependence of magnetic susceptibility in the lower temperature region. From these results, UO_2 is deduced to be magnetically diluted mainly with diamagnetic Ce^{4+} ions, because if all cerium ions were in the +3 state (paramagnetic state), the decrease of T_N , which is the indication of the magnetic dilution of UO_2 would no longer be observed. In fact, for $(\text{U}, \text{Pr})\text{O}_2$ and $(\text{U}, \text{Nd})\text{O}_2$

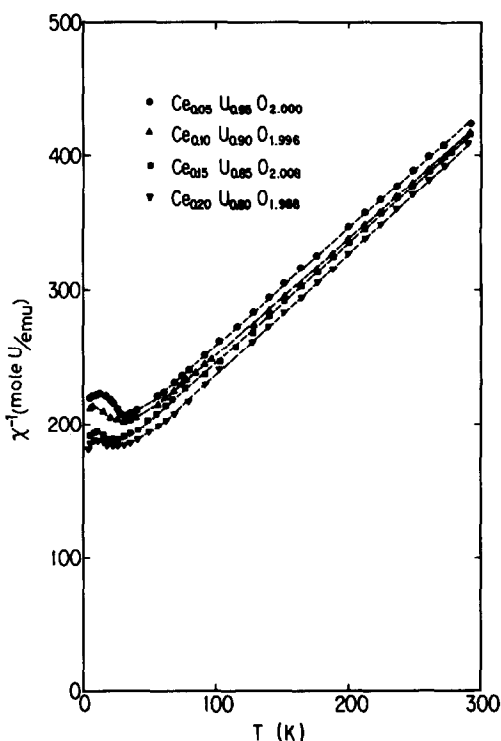


FIG. 2. Temperature dependence of inverse-magnetic susceptibilities per mole of uranium for the solid solutions with $y \leq 0.20$.

solid solutions (18, 19) a discontinuous change was found just below T_N in the magnetic susceptibility vs temperature curve, and T_N did not decrease with decreasing uranium concentration.

A consistent result can be drawn from the magnitude of the paramagnetic susceptibility and its dependence on cerium concentration. Figures 2 and 3 show that the inverse magnetic susceptibility of uranium decreases with increasing cerium concentration over the paramagnetic temperature range examined. This behavior is the same as that found in $(U, Th)O_2$ (14) or $(U, Th, Zr)O_2$ (24) solid solutions, and it is different from that found in $(U, Y)O_2$ (16) or $(U, La)O_2$ (17) solid solutions. The susceptibility per mole of uranium for the $(U, Y)O_2$ or $(U, La)O_2$ solid solutions decreased with

increasing concentration of diamagnetic diluents in the temperature range in which the Curie-Weiss law holds. This fact indicates that, with increasing amount of trivalent diluents, the amount of uranium ions oxidized from the tetravalent to the pentavalent state increases, which results in a decrease of magnetic moment (magnetic susceptibility) of uranium overall. Therefore, the case that all the Ce^{4+} are reduced to Ce^{3+} state in the solid solutions can be excluded.

Below the transition temperature, the magnetic susceptibility decreased with decreasing temperature and then increased again (see Figs. 4 and 5), which is different from the behavior found in $(U, Th)O_2$ (14) or $(U, Th, Zr)O_2$ (24) solid solutions where the magnetic susceptibilities attained to constant values below the Néel tempera-

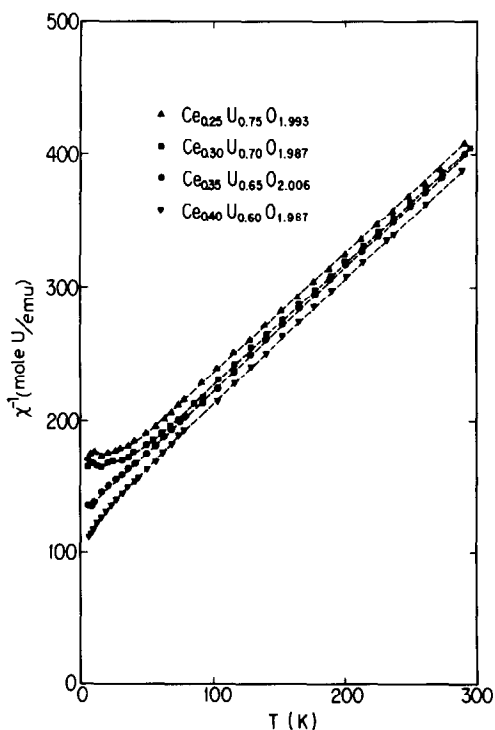


FIG. 3. Temperature dependence of inverse-magnetic susceptibilities per mole of uranium for the solid solutions with $y \geq 0.25$.

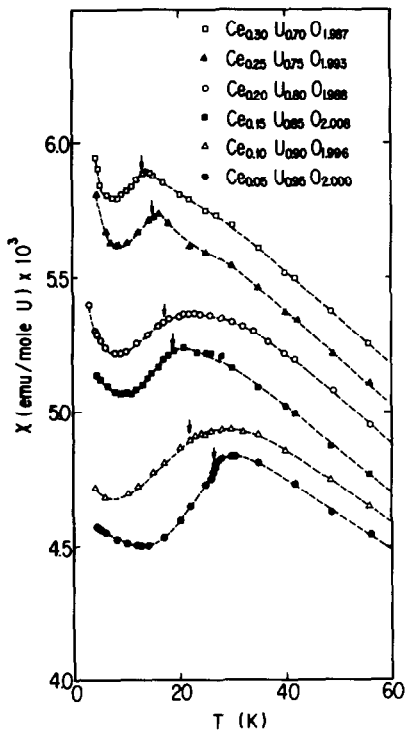


FIG. 4. Temperature dependence of magnetic susceptibilities for the solid solutions with $y \leq 0.30$ at low temperatures. Arrows show the Néel temperatures.

ture. The behavior found in $(U, Ce)O_2$ solid solutions may also be contrasted to that in $(U, Y)O_2$ (16) or $(U, La)O_2$ (17) solid solutions where, below T_N , the magnetic susceptibilities decreased with decreasing temperature, which is normal for an antiferromagnet. For comparison, the magnetic susceptibility data of $Th_{0.10}U_{0.90}O_{2.000}$, $Y_{0.10}U_{0.90}O_{2.002}$, $La_{0.10}U_{0.90}O_{2.005}$, and $Pr_{0.03}U_{0.97}O_{1.998}$ are depicted together in Fig. 6. If a paramagnetic impurity is contained in an antiferromagnet, the magnetic susceptibility would increase with decreasing temperature below T_N . Since the step-like decline of the susceptibility has been observed to be very sharp for UO_2 when the temperature is lowered through T_N (13, 25, 26), small amounts of the paramagnetic impurity would not change the Néel temperature (18). In $(U, Ce)O_2$ solid solutions, the Néel

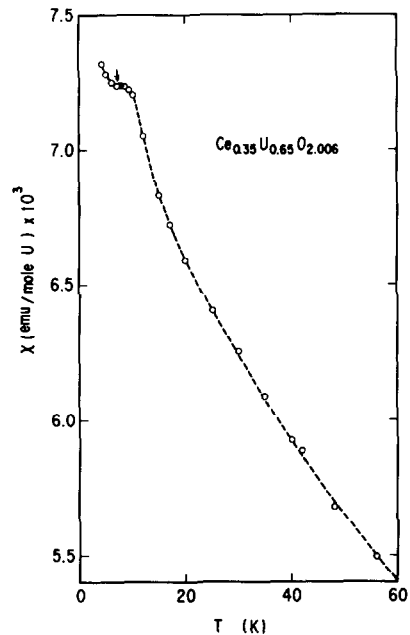


FIG. 5. Temperature dependence of magnetic susceptibility for $Ce_{0.33}U_{0.65}O_{2.006}$ at low temperatures. Arrow shows the Néel temperature.

temperature decreased with increasing cerium concentration, i.e., the paramagnetic impurity need not be considered. The increase of magnetic susceptibility below T_N

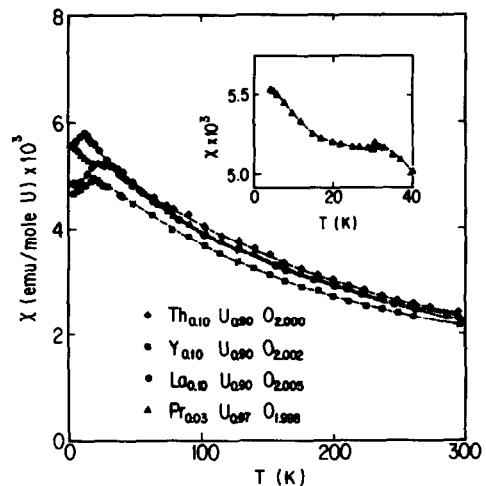


FIG. 6. Magnetic susceptibilities of $L_yU_{1-y}O_2$ ($L = Th, Y, La, Pr$) solid solutions.

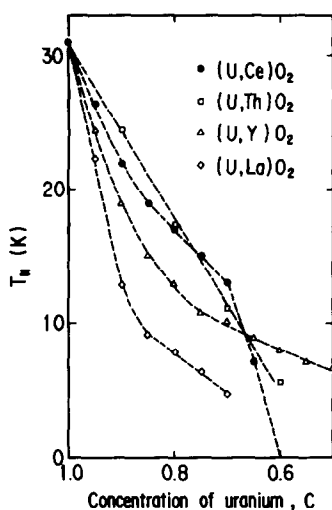


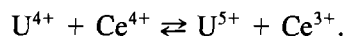
FIG. 7. Variation of Néel temperature with uranium concentration.

is then considered to be characteristic of $(U, Ce)O_2$ solid solutions. Such increase becomes more prominent with cerium concentration (Fig. 4).

3. Néel Temperature

The Néel temperature was plotted against uranium concentration in Fig. 7. It decreases gradually with decreasing uranium concentration (C) down to $C = 0.70$. Below that concentration it decreases more rapidly ($T_N = 7.1$ K for $U_{0.65}Ce_{0.35}O_2$) until $C = 0.60$ at which no antiferromagnetic transition is observed in the experimental temperature range (Fig. 3). For comparison, the data for $(U, Th)O_2$ (14), $(U, Y)O_2$ (16), and $(U, La)O_2$ (17) solid solutions are also drawn in Fig. 7. The Néel temperature curve for the $(U, Ce)O_2$ solid solutions is different from those of the above solid solutions. For $(U, Th)O_2$ and $(U, Zr)O_2$ solid solutions (15), the Néel temperature decreases linearly with decreasing uranium concentration. This behavior is qualitatively in accord with the theoretical prediction except for that around the critical concentration at which antiferromagnetism

disappears (27–33). The nonlinear dependence of the Néel temperatures on uranium concentration found for $(U, Y)O_2$ and $(U, La)O_2$ solid solutions has been understood as related to the formation of U^{5+} ions (16). From both the results of the nonlinear dependence of Néel temperature on uranium concentration (see Fig. 7) and the increase of magnetic susceptibility below T_N (see Figs. 4 and 5), which will be discussed in a later section, we consider that in the $(U, Ce)O_2$ solid solutions, some transfer of electrons occurs between uranium and cerium ions, i.e., some of the uranium ions are oxidized and a corresponding number of cerium ions are reduced. In this case, the oxidation states of uranium and cerium may be represented by the equilibrium reaction,



If this charge transfer proceeds completely (all the Ce^{4+} ions are reduced to Ce^{3+} state), the so-called magnetic dilution does not occur because of the paramagnetism of the Ce^{3+} ion, as mentioned above. In $(U, Pr)O_2$ solid solutions, the oxidation state of the praseodymium ion remains +3 (paramagnetic) and some uranium ions are oxidized to the +5 state according to the charge neutrality condition (18, 34). In the magnetic susceptibility vs temperature curve of $(U, Pr)O_2$ solid solutions with low Pr concentrations ($Pr/(Pr + U) \leq 0.07$), the susceptibility showed a discontinuous drop at ca. 30–31 K (see Fig. 6), and this temperature was constant irrespective of praseodymium concentration (18). In the $(U, Ce)O_2$ solid solutions, the Néel temperature decreases with increasing cerium concentration. Therefore, the charge transfer reaction described by the above equation is considered to occur partly between uranium and cerium ions.

From a comparison of the data of $(U, Y)O_2$ and $(U, La)O_2$ solid solutions with those of $(U, Th)O_2$, it can be said that the

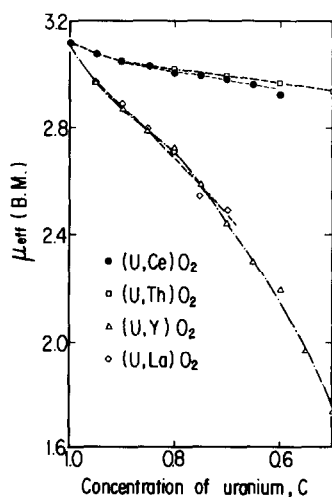


FIG. 8. Variation of magnetic moment of uranium with uranium concentration.

Néel temperature drastically decreases if the U^{5+} ions increase in the solid solutions. The rapid decrease of the Néel temperature of $(U, Ce)O_2$ solid solutions below $C = 0.70$ is considered to be, as one possibility, due to the occurrence of the charge transfer to a larger extent in this concentration range.

As mentioned above, the magnetic susceptibility of $(U, Ce)O_2$ solid solutions increases with decreasing temperature at very low temperatures below T_N , and this trend becomes more prominent as the cerium concentration increases. The increase of magnetic susceptibility below T_N is considered to be due to an increased concentration of Ce^{3+} ions, and not to the U^{5+} ions, because the magnetic interactions between $U^{5+}-U^{5+}$ ions (or in some cases those between $U^{5+}-U^{4+}$ ions) in the fluorite structure diminish the magnetic susceptibility below T_N , as shown in the case of $(U, Y)O_2$ (16) or $(U, La)O_2$ (17) solid solutions. The Ce^{3+} ion is a Kramers' ion having one unpaired $4f$ electron and its ratio in the cerium ions is likely to increase with cerium concentration.

By extrapolating the two sets of data of the Néel temperature for $y = 0.30$ and $y =$

0.35, the critical concentration of $(U, Ce)O_2$ solid solutions at which antiferromagnetism disappears was estimated to be $y = 0.40$, as shown in Fig. 7.

4. Magnetic Moment

From the inclination of the reciprocal susceptibility vs temperature curves, the effective magnetic moments were obtained in the temperature region where the Curie-Weiss law holds. The variation of magnetic moment with uranium concentration is shown in Fig. 8. For comparison, the data for $(U, Th)O_2$ (14), $(U, Y)O_2$ (16), and $(U, La)O_2$ (17) solid solutions are also plotted. The magnetic moment decreases with decreasing uranium concentration. The decrement of $(U, Ce)O_2$ is comparable with that of $(U, Th)O_2$ solid solutions and is less than that of $(U, Y)O_2$ or $(U, La)O_2$ solid solutions. As discussed earlier (14), the decrease of magnetic moment in the $(U, Th)O_2$ solid solutions is responsible for the decrease of the magnetic interactions between the adjacent uranium ions. On the other hand, the decrease of magnetic moment in the $(U, Y)O_2$ or $(U, La)O_2$ solid solutions is due to the formation of U^{5+} ion which gives lower magnetic moment than U^{4+} ion (16, 17). From the similarity of magnetic moment of $(U, Ce)O_2$ solid solutions to that of $(U, Th)O_2$ solid solutions, the slight decrease of the magnetic moment of $(U, Ce)O_2$ solid solutions with decreasing uranium concentration is considered to be mainly due to the decrease in the magnetic interactions between the adjacent uranium ions. The fact that the Néel temperature decreases with decreasing uranium concentration supports this conclusion. In the former sections, we have discussed that some uranium ions in the $(U, Ce)O_2$ solid solutions are oxidized to the pentavalent state. However, this effect is not reflected in the decrease of magnetic moment of uranium. This is because the effective magnetic moment obtained from the inclination

of inverse-magnetic susceptibility vs temperature curve gives the sum of the moments of uranium and Ce^{3+} ions when the electron charge transfer occurs between the uranium and cerium ions ($U^{4+} + Ce^{4+} \rightleftharpoons U^{5+} + Ce^{3+}$), and because the total moment of U^{5+} and Ce^{3+} is near to that of U^{4+} .¹

References

1. K. A. HOFMANN AND K. HÖSCHELE, *Ber. Dtsch. Chem. Ges.* **48**, 20 (1915).
2. V. W. RÜDORFF AND G. VALET, *Z. Anorg. Allg. Chem.* **271**, 257 (1953).
3. V. G. BRAUER AND R. TIESSLER, *Z. Anorg. Allg. Chem.* **271**, 273 (1953).
4. M. B. ROBIN AND P. DAY, *Adv. Inorg. Chem. Radiochem.* **10**, 400 (1967).
5. T. L. MARKIN, R. S. STREET, AND E. C. CROUCH, *J. Inorg. Nucl. Chem.* **32**, 59 (1970).
6. T. L. MARKIN AND E. C. CROUCH, *J. Inorg. Nucl. Chem.* **32**, 77 (1970).
7. R. LORENZELLI AND B. TOUZELIN, *J. Nucl. Mater.* **95**, 290 (1980).
8. H. TAGAWA, T. FUJINO, K. WATANABE, Y. NAKAGAWA, AND K. SAITA, *Bull. Chem. Soc. Japan* **54**, 138 (1981).
9. D. I. R. NORRIS AND P. KAY, *J. Nucl. Mater.* **116**, 184 (1983).
10. H. P. NAWADA, P. SRIRAMAMURTI, K. V. GOVINDAN KUTTY, S. RAJAGOPALAN, R. B. YADAV, P. R. VASUDEVA RAO, AND C. K. MATHEWS, *J. Nucl. Mater.* **139**, 19 (1986).
11. T. B. LINDERMER AND J. BRYNESTAD, *J. Amer. Ceram. Soc.* **69**, 867 (1986), and references therein.
12. B. C. FRAZER, G. SHIRANE, D. C. COX, AND C. E. OLSEN, *Phys. Rev.* **140**, A1448 (1965).
13. J. B. COMLY, *J. Appl. Phys.* **39**, 716 (1968).
14. Y. HINATSU AND T. FUJINO, *J. Solid State Chem.* **60**, 195 (1985).
15. Y. HINATSU AND T. FUJINO, *J. Solid State Chem.* **60**, 244 (1985).
16. Y. HINATSU AND T. FUJINO, *J. Solid State Chem.* **66**, 332 (1987).
17. Y. HINATSU AND T. FUJINO, *J. Solid State Chem.* **68**, 255 (1987).
18. Y. HINATSU AND T. FUJINO, *J. Solid State Chem.*, in press.
19. Y. HINATSU AND T. FUJINO, *J. Solid State Chem.* **73**, 388 (1988).
20. L. V. AZAROFF, "Elements of X-ray Crystallography," p. 479, McGraw-Hill, New York (1968).
21. S. R. DHARWADKAR AND M. S. CHANDRASEKHARAIH, *Anal. Chim. Acta* **45**, 545 (1969).
22. T. FUJINO AND T. YAMASHITA, *Fresenius' Z. Anal. Chem.* **314**, 156 (1983).
23. L. L. SPARKS AND R. L. POWELL, *J. Res. Nat. Bur. Stand. U.S.* **A76**, 263 (1972).
24. Y. HINATSU AND T. FUJINO, *J. Solid State Chem.* **63**, 250 (1986).
25. M. J. M. LEASK, L. E. ROBERTS, A. J. WALTER, AND W. P. WOLF, *J. Chem. Soc.*, 4788 (1963).
26. A. ARROTT AND J. E. GOLDMAN, *Phys. Rev.* **108**, 948 (1957).
27. H. SATO, A. ARROTT, AND R. KIKUCHI, *J. Phys. Chem. Solids* **10**, 19 (1959).
28. R. J. ELLIOTT, *J. Phys. Chem. Solids* **16**, 165 (1961).
29. J. S. SMART, *J. Phys. Chem. Solids* **16**, 169 (1961).
30. R. J. ELLIOTT AND B. R. HEAP, *Proc. R. Soc. London Ser. A* **265**, 264 (1961).
31. G. S. RUSHBROOKE AND D. J. MORGAN, *Mol. Phys.* **4**, 1 (1961).
32. C. DOMB AND N. W. DALTON, *Proc. Phys. Soc.* **89**, 856 (1966).
33. D. J. MORGAN AND G. S. RUSHBROOKE, *Mol. Phys.* **4**, (1961).
34. T. YAMASHITA AND T. FUJINO, *J. Nucl. Mater.* **132**, 192 (1985).

¹ If the magnetic moment of U^{3+} and Ce^{3+} are 2.00 and 2.54 B.M., respectively, the total moment is calculated to be 3.2 B.M., which is near to the moment of UO_2 (Y. Hinatsu and T. Fujino, to be submitted).